

Action Noise in Off-Policy Deep Reinforcement Learning: Impact on Exploration and Performance

Jakob Hollenstein

Department of Computer Science, University of Innsbruck

jakob.hollenstein@uibk.ac.at

Sayantan Auddy

Department of Computer Science, University of Innsbruck

sayantan.auddy@uibk.ac.at

Matteo Saveriano

Department of Industrial engineering, University of Trento

matteo.saveriano@unitn.it

Erwan Renaudo

Department of Computer Science, University of Innsbruck

erwan.renaudo@uibk.ac.at

Justus Piater

Department of Computer Science, University of Innsbruck

justus.piater@uibk.ac.at

Abstract

Many deep reinforcement learning algorithms rely on simple forms of exploration, such as the additive action-noise often used in continuous control domains. Typically, the scaling factor of this action noise is chosen as a hyper-parameter and kept constant during training. In this paper, we analyze how the learned policy is impacted by the noise type, scale, and reducing of the scaling factor over time. We consider the two most prominent types of action-noise: Gaussian and Ornstein-Uhlenbeck noise, and perform a vast experimental campaign by systematically varying the noise type and scale parameter, and by measuring variables of interest like the expected return of the policy and the state space coverage during exploration. For the latter, we propose a novel state-space coverage measure $X_{\mathcal{U}_{\text{rel}}}$ that is more robust to boundary artifacts than previously proposed measures. Larger noise scales generally increase state space coverage. However, we found that increasing the space coverage using a larger noise scale is often not beneficial. On the contrary, reducing the noise-scale over the training process reduces the variance and generally improves the learning performance. We conclude that the best noise-type and scale are environment dependent, and based on our observations, derive heuristic rules for guiding the choice of the action noise as a starting point for further optimization.

Contents

1 Introduction

In (deep) reinforcement learning an agent aims to learn a policy to act optimally based on data it collects by interacting with the environment. In order to learn a well performing policy, data — state-action-reward sequences — of sufficiently good behavior need to be collected. A simple and very common method to discover better data, is to induce variation in the data collection by adding action noise to the action selection process.

Through this variation, the agent will try a wide range of action sequences and eventually discover useful information.

Action Noise In off-policy reinforcement learning algorithms applied to continuous control domains, a go-to approach is to add a randomly sampled *action noise* to the action chosen by the policy. Typically the action

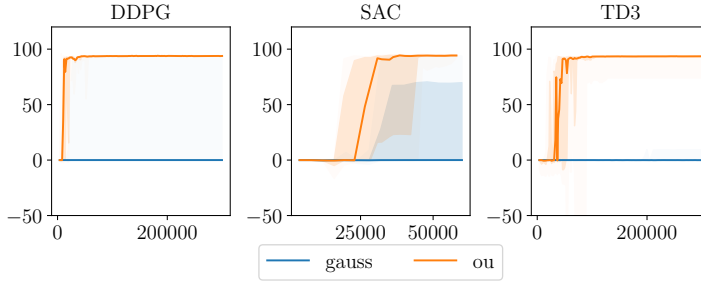


Figure 1: Mountain-Car: all algorithms trained according to the tuned parameters found by Raffin (2020) with the exception of action noise. In case of SAC also external noise is added to the action. The lines indicate the medians, the shaded areas the quartiles of ten independent runs.

Noise-Type	Gaussian	Ornstein-Uhlenbeck
Scale	0.60	0.50
Return	-30.24	-30.37
+-	0.13	1.32

Table 1: Example: Mountain-Car, driving the environment by different noise types, σ chosen to yield similar returns;

noise is sampled from a Gaussian distribution or an Ornstein-Uhlenbeck process, either because algorithms are proposed using these noise types (Fujimoto et al., 2018; Lillicrap et al., 2016), or because these two types are provided by reinforcement learning implementations (Liang et al., 2018; Raffin et al., 2021a; Fujita et al., 2021; Seno and Imai, 2021). While adding action noise is a simple, widely used and surprisingly effective approach, the impact of action noise type or scale does not feature very prominently in the reinforcement learning literature. However, the action noise can have a huge impact on the learning performance as the following example shows.

A motivating example Consider the case of the *Mountain-Car* (Moore, 1990) environment.

In this task, a car starts in a valley between mountains on the left and right and does not have sufficient power to simply drive up the mountain. It needs repetitive swings to increase its potential and kinetic energy to finally make it up to the top of the mountain on the right side. The actions apply a force to the car and incur a cost that is quadratic to the amount of force, while reaching the goal yields a final reward of 100. This parameterization implies a local optimum: not performing any action and achieving a return of zero.

We apply the algorithms DDPG, TD3 and SAC (Lillicrap et al., 2016; Fujimoto et al., 2018; Haarnoja et al., 2019) to this task and use two types of action noise, Gaussian and Ornstein-Uhlenbeck. The action is generated as $a_t = \pi_\theta(s_t) + \varepsilon_{a_t}$, where ε_{a_t} denotes the action noise. We calibrate the noise-scale to achieve similar returns for both noise types. To calibrate, we assume a constant-zero-action policy upon which the action noise is added and effectively use $a_t = \varepsilon_{a_t}$ as the action sequence. We find that a scale of about 0.6 for Gaussian action noise and a scale of about 0.5 for Ornstein-Uhlenbeck noise lead to a mean return of about -30 . A successful solution to the Mountain-Car environment yields a positive return $0 < \sum r_t < 100$. This is shown in Table 1. We then use these two noise-configurations and perform learning with DDPG, SAC and TD3. The resulting learning curves are shown in Figure 1 and very clearly depict the huge impact the noise configuration has: with similar returns of the noise-only policies, we achieve substantially different learning results, either leading to failure or success on the task.

To achieve a swing-up, the actions must not change direction too rapidly but rather need to change direction with the right frequency. Ornstein-Uhlenbeck noise is temporally correlated and thus helps solving the environment successfully at a smaller scale. In this environment, the algorithms tend to converge either to the successful solution of the environment by swinging up, or to a passive zero-action solution which incurs no penalty.

Relation to ε -greedy

A very common strategy in Q-learning algorithms applied to discrete control, is to select a random action with a certain probability ε . In this *epsilon-greedy* strategy, the probability ε is often chosen higher in the beginning of the training process and reduced to a smaller value over course of the training. Although very common in Q-learning, a comparable strategy has not received a lot of attention for action noise in continuous

control. The most prominent algorithms using action noise, namely DDPG (Lillicrap et al., 2016) and TD3 (Fujimoto et al., 2018), do not mention changing the noise over the training process. Another prominent algorithm, SAC (Haarnoja et al., 2019), adapts the noise to an entropy target. The entropy target, however, is kept constant over the training process. In many cases the optimal policy would be deterministic, but the agent has to behave with similar average action-entropy no matter whether the optimal policy has been found or not. Another indication that this has received little attention is that only very few reinforcement learning implementations, e.g., RLlib (Liang et al., 2018), implement reducing the impact of action noise over the training progress. Some libraries, like `coach` (Caspi et al., 2017), only implement a form of continuous epsilon greedy: sampling the action noise from a uniform distribution with probability ε . The majority of available implementations, including `stable-baselines` (Raffin et al., 2021a), `PFRL` (Fujita et al., 2021), `acme` (Hoffman et al., 2020), and `d3rlpy` (Seno and Imai, 2021), do not implement any strategies to reduce the impact of action noise over the training progress.

Findings In this paper we analyze the impact of Gaussian and Ornstein-Uhlenbeck noise on the learning process of DDPG, TD3, SAC and a deterministic SAC variant. Evaluation is performed on the Mountain-Car (Brockman et al., 2016) environment from the OpenAI Gym, and Inverted-Pendulum-Swingup, Reacher, Hopper, Walker2D and Half-Cheetah environments implemented using PyBullet (Coumans and Bai, 2016; Ellenberger, 2018) (described in Table 2).

We found that the noise configuration, noise-type & noise-scale, have an important impact and can be necessary for learning (e.g. Mountain-Car) or break learning (e.g. Hopper). Larger noise scales tend to increase state space coverage, but for the majority of our investigated environments increasing the state space coverage is not beneficial.

We found that across noise configurations, decaying tends to work better than constant noise, in both reducing the variance across seeds and improving the learned policy performance and can thus make the algorithms more robust to the action-noise hyper-parameter.

1.1 Contributions

In this paper, we analyze the effect of the two most prominent action noise types (Ornstein-Uhlenbeck, Gaussian) and different noise scales (0.1, 0.5, 0.9, 1.3) on the evaluation performance, the exploratory returns and the exploratory state space coverage.

- We perform a vast experimental study and investigate the question whether one of the two noise-types is preferable, whether a specific scale should be used and whether there is any benefit to reducing the scale over the training progress (linearly, logistically) compared to keeping it constant.
- We investigate the relation between state space coverage and learned policy performance.
- We propose to assess the state space coverage using our novel measure $X_{\mathcal{U}_{\text{rel}}}$ that is more robust to approximation artifacts on bounded spaces compared to previously proposed measures.

2 Related Work

Ever since Mnih et al. (2015) were able to show substantial improvements on the Atari Games RL benchmarks (Bellemare et al., 2013) by combining Deep Learning with Reinforcement Learning in their DQN method, the interest in Deep Reinforcement Learning has been rising.

Robotics: In robotics, the interest in deep reinforcement learning has also been rising and common benchmarks are provided by the OpenAI Gym (Brockman et al., 2016), which includes control classics such as the Mountain-Car environment (Moore, 1990) as well as more complicated (robotics) tasks based on the MuJoCo simulator (Todorov et al., 2012). Another common benchmark is the DM Control Suite (Tassa et al., 2018), also based on MuJoCo. While MuJoCo has seen widespread adoption it was, until recently, not freely available. A second popular simulation engine, that has been freely available, is the Bullet simulation engine (Coumans and Bai, 2016) and very similar benchmark environments are also available for the Bullet engine (Coumans and Bai, 2016; Ellenberger, 2018).

Continuous Control:

While the Atari games feature large and (approximately) continuous observation spaces, their action spaces are discrete and relatively small, making Q-learning a viable option. In contrast, typical robotics tasks require *continuous action spaces*, implying uncountable many different actions. A tabular Q-learning approach is therefore not possible and maximizing the action over a learned function approximator for $Q(s, a)$ is computationally expensive (although not impossible as Kalashnikov et al. (2018) have shown). Therefore, in continuous action spaces, *policy search* is employed, to directly optimize a function approximator *policy*, mapping from state to best performing action (Williams, 1992). To still reap the benefits of reduced sample complexity of TD-methods, policy search is often combined with learning a value function, a *critic*, leading to an *actor-critic* approach (Sutton et al., 1999).

On- and Off-policy: Current state of the art D-RL algorithms consist of *on-policy* methods, such as TRPO (Schulman et al., 2015) or PPO (Schulman et al., 2017), and *off-policy* methods, such as DDPG (Lillicrap et al., 2016), TD3 (Fujimoto et al., 2018) and SAC (Haarnoja et al., 2019). While the on-policy methods optimize the next policy iteration with respect to the data collected by the current policy, off-policy methods are, apart from stability issues and requirements on the samples, able to improve policy performance based on data collected by *any arbitrary* policy and thus can also re-use older samples.

To improve the policy, variation (*exploration*) in the collected data is necessary. The most common form of exploration is based on randomness: in on-policy methods this comes from a *stochastic policy* (TRPO, PPO), while in the off-policy case it is possible to use a stochastic policy (SAC) or, to use a *deterministic policy* (Silver et al., 2014) with added *action noise* (DDPG, TD3). Since off-policy algorithms can learn from data collected by other policies, it is also possible to combine stochastic policies (e.g. SAC) with action noise.

State-Space Coverage: Often, the reward is associated with reaching certain areas in the state space. Thus, in many cases, *exploration* is related to *state-space coverage*. An intuitive method to calculate state space coverage is based on binning the state space and counting the percentage of non-empty bins. Since this requires exponentially many points as the dimensionality increases, other measures are necessary. Zhan et al. (2019) propose to measure state coverage by drawing a bounding box around the collected data and measuring the means of the side-lengths, or by measuring the sum of the eigenvalues of the estimated covariance matrix of the collected data. However, so far, there is no common and widely adopted approach.

Methods of Exploration: The architecture for the stochastic policy in SAC (Haarnoja et al., 2019), consists of a neural network parameterizing a Gaussian distribution, which is used to sample actions and estimate action-likelihoods. A similar stochastic policy architecture is also used in TRPO (Schulman et al., 2015) and PPO (Schulman et al., 2017). While this is the most commonly used type of distribution, more complicated parameterized stochastic policy distributions based on normalizing flows have been proposed (Mazoure et al., 2020; Ward et al., 2019). In case of action noise, the noise processes are not limited to uncorrelated Gaussian (e.g. TD3) and temporally correlated Ornstein-Uhlenbeck noise (e.g. DDPG): a whole family of action noise types is available under the name of colored noise, which has been successfully used to improve the Cross-Entropy-Method (Pinneri et al., 2020). A quite different type of random exploration are the parameter space exploration methods (Mania et al., 2018; Plappert et al., 2017), where noise is not applied to the resulting action, but instead, the parameters of the policy are varied. As a somewhat intermediate method, state dependent exploration (Raffin et al., 2021b) has been proposed, where action-“noise” is deterministic-ally generated by a function based on the state. Here, the function parameters are changed randomly for each episode, leading to different “action-noise” for each episode. Presumably among the most intricate methods to generate exploration are the methods that train a policy to achieve exploratory behavior by rewarding exploratory actions (Burda et al., 2019; Tang et al., 2017; Mutti et al., 2020; Hong et al., 2018; Pong et al., 2020).

It is however, not clear yet, which exploration method is most beneficial, and when a more complicated method is actually worth the additional computational cost and complexity. In this work we aim to reduce this gap, by investigating the most widely used baseline method in more detail: exploration by action noise.

3 Methods

In this section, we describe the action-noise types, the schedulers to reduce the impact of the action noise over time and the evaluation process in more detail. We briefly list the analyzed benchmark environments and their most important properties. We chose environments of increasing complexity that model widely used benchmark tasks. We list the used algorithms and then describe how we gather evaluation data and how it is aggregated. Last, we describe the methods we use for analyzing state space coverage.

3.1 Noise-Types: Gaussian and Ornstein-Uhlenbeck

The action-noise ε_{a_t} is added to the action drawn from the policy:

$$a_t = \tilde{a}_t + \beta \text{clip}_{[-1;1]}[\varepsilon_{a_t}] \cdot \frac{a_{\max} - a_{\min}}{2} + \frac{a_{\max} + a_{\min}}{2} \quad (1)$$

where $\tilde{a}_t \sim \pi_\theta(s_t)$ for stochastic policies or $\tilde{a}_t = \pi_\theta(s_t)$ for deterministic policies. We introduce an additional scaling-ratio β , which is typically kept constant at the value one. In the next section we describe how we change β over time.

The action noise ε_{a_t} is drawn from either a Gaussian distribution or an Ornstein-Uhlenbeck (OU) process. The noise distributions are factorized, i.e. noise samples are drawn independently for each action dimension. The actions are assumed to be defined on the interval $[-1, 1]$, generated action-noise samples are clipped to this interval, and then rescaled and shifted to fit the actual action limits defined by the environment. The resulting action a_t is also clipped to the action limits defined by the environment.

Gaussian noise is temporally uncorrelated and is typically applied on symmetric action spaces (Hill et al., 2018; Raffin, 2020) with commonly used values of $\mu = 0$ and $\sigma = 0.1$ with $\Sigma = \mathbf{I} \cdot \sigma$. Action noise is sampled according to

$$\varepsilon_{a_t} \sim \mathcal{N}(\mu, \Sigma) \quad (2)$$

Ornstein-Uhlenbeck noise is sampled from the following temporal process, with each action dimension calculated independently of the other dimensions:

$$\varepsilon_{a_t} = \varepsilon_{a_{t-1}} + \theta(\mu - \varepsilon_{a_{t-1}}) \cdot dt + \sigma \sqrt{dt} \cdot \epsilon_t \quad (3)$$

$$\varepsilon_{a_0} = \mathbf{0} \quad \epsilon_t \sim \mathcal{N}(\mathbf{0}, \mathbf{I}) \quad (4)$$

The parameters we use for Ornstein-Uhlenbeck noise are taken from a widely used RL-algorithm implementation (Hill et al., 2018): $\theta = 0.15$, $dt = 0.01$, $\mu = 0 \cdot \mathbf{1}$, $\sigma = 0.1 \cdot \mathbf{I}$.

Due to the huge number of possible combinations of environments, algorithms, noise-type, noise-scale and the necessary repetition with different seeds, we had to limit the number of investigated scales. We set out with two scales encountered in pre-tuned hyper-parameterization (Raffin, 2020) and continued with a linear increase: 0.1, 0.5, 0.9, 1.3, 1.7

Because the action noise is clipped to $[-1, 1]$ before being scaled to the actual action limits, a very large scale, such as 1.7 implies a larger percentage of on-the-boundary action noise samples and is thus more similar to bang-bang control style actions. This is interesting because bang-bang style control has been found surprisingly effective for many RL benchmarks (Seyde et al., 2021).

3.2 Scheduling strategies to reduce action noise

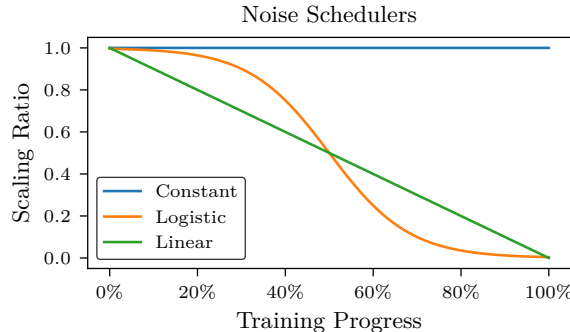


Figure 2: Different schedulers to reduce impact of action noise over time. Similar to ϵ -greedy strategies in discrete-action Q-learning, the logistic and linear schedulers reduce the impact of noise over the course of the training progress, where training process denotes the fraction of training-steps-completed divided by the total number of training steps.

In (1) we introduce the action-noise scaling-ratio β . In this work we compare a constant-, linear- and logistic-scheduler for the value of β . The effective scaling of the action noise by the noise schedulers is illustrated in Figure 2. The noise types are described in more detail in Section 3.1.

Changing the σ (see (3) and (2)) instead of β could result in a different shape of the distribution, for example when values are clipped, or when the σ indirectly affects the result as in the Ornstein-Uhlenbeck process.

To keep the shape constant, the action noise schedulers do not change the σ parameter of the noise process but instead scale down the resulting sampled action-noise values by changing the β parameter: this means that the effective range of the action noise, before scaling and adjusting to the environment limits, changes over time from $[-1, 1]$, the maximum range, to $[-0, 0]$ for the linear and logistic schedulers.

3.3 Environments

For evaluation we use various environments (Brockman et al., 2016; Coumans and Bai, 2016; Ellenberger, 2018) of increasing complexity. Table 2 lists the observation- and action-space dimensionalities along an illustration of the environment. A rough sketch of the reward is also provided to indicate whether the reward is sparse or dense with respect to a goal state, goal region, or a change of the distance to the goal region. It also indicates what kind of penalties, if any, apply: many environments feature linear or quadratic (energy) penalties on the actions, sparse penalties on the state or part of the state (such as joint limits), dense penalties, for example based on forces or required power induced by joint states. For brevity the descriptions do not include factors associated with the terms and the exact calculations, see (Brockman et al., 2016; Coumans and Bai, 2016; Ellenberger, 2018) for the exact reward formulations.

3.4 Performed experiments

We evaluate using the algorithms TD3 (Fujimoto et al., 2018), DDPG (Lillicrap et al., 2016), SAC (Haarnoja et al., 2019), and a deterministic version of SAC (DetSAC, Algorithm A.1). Originally SAC was proposed with only exploration from its stochastic policy. However, since SAC is an off-policy algorithm, it is possible to add additional action noise, a common solution for environments such as the Mountain Car. The stochastic policy in SAC typically is a parameterized gaussian and adding additional action noise to the actions sampled from the stochastic policy could impact the results. Thus, we also compare to our DetSAC version, where action-noise is added to the maximum likelihood action of the DetSAC policy (Algorithm A.1).

We use the implementations provided by Raffin et al. (2021a), following the hyper-parameterizations provided by Raffin (2020), but adapting the action-noise settings.

ENVIRONMENT	ILLUSTRATION	$ \mathcal{O} $	$ \mathcal{A} $	REWARD
Mountain-Car		2	1	$\mathbf{1}(s_t, s_G) - a_t _2^2$
Inverted-Pendulum-Swingup		5	1	$ \varphi(s_t) - \varphi_G _1$
Reacher		9	2	$\nabla^- s_t - s_G _2 - \varphi(s_t) _2^2 - \mathbf{1}(\varphi(s_t), \varphi_{\text{limit}}) - a_t _1$
Hopper		15	3	$\nabla^- s_t - s_G _1 - \varphi(s_t) _2^2 - \mathbf{1}(\varphi(s_t), \varphi_{\text{limit}}) - a_t _1$
Walker2D		22	6	$\nabla^- s_t - s_G _1 - \varphi(s_t) _2^2 - \mathbf{1}(\varphi(s_t), \varphi_{\text{limit}}) - a_t _1$
Half-Cheetah		26	6	$\nabla^- s_t - s_G _1 - \varphi(s_t) _2^2 - \mathbf{1}(\varphi(s_t), \varphi_{\text{limit}}) - a_t _1$

Table 2: Illustrations of the benchmark environments used in the evaluation. Observation space and Action space dimensionalities are listed, along an illustration of the environment. A rough sketch of the reward: $\mathbf{1}(b, c)$ indicator function (sparse reward or penalty) of b w.r.t. to the set c , $|b|_n$ n-norm of b , $\varphi(s_t)$ angular component of state, $\nabla^- b$ finite-difference reduction of b between time-steps, φ_{max} joint limit, s_G goal state, $|\varphi(s_t)|_2^2$ denotes an angular-power-penalty, factors in the reward are omitted, distances e.g. $|s_t - s_G|_n$ may refer to a subspace of the vector s_t .

Each experiment is repeated multiple times with different seeds: by repeating each experiment with 20 seeds the total number amounts to 14400 experiments. On a single node, AMD Ryzen 2950X equipped with four GeForce RTX 2070 SUPER, 8 GB, running about twenty experiments in parallel this would amount to a runtime of approximately 244 node-days. Since multiple nodes were available, we were able to run the experiments over the course of about eight weeks.

Table C.1 lists the number of independent runs performed for each experimental configuration.

3.5 Measuring Performance

We divide the learning process into 100 segments and evaluate the exploration and learned policy performance once for each of those segments: at the end of each segment, we perform evaluation rollouts for 100 episodes or 10000 steps, whichever is reached first, using only complete episodes. We perform evaluation rollouts to assess the performance of the learned policy — deterministic or maximum likelihood actions — without action noise. The learning algorithms use a replay buffer and we can assess the achieved reward and exploration of the collected data based on the replay buffer. Since the content of the replay buffer is changing slowly, evaluation based on the replay buffer are temporally smoothed. Thus changes in the exploration only become visible gradually.

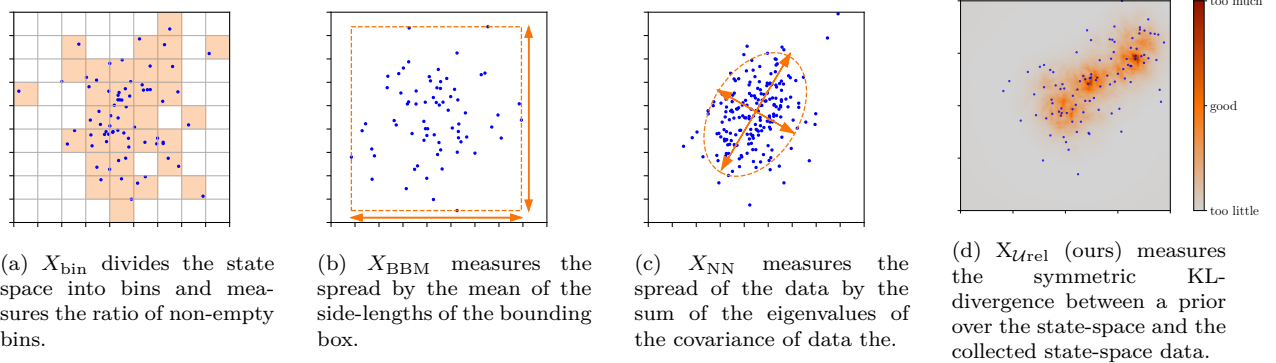


Figure 3: Illustrations of the state space coverage measures.

To see changes in the exploration more quickly, we perform noisy (exploratory) evaluation rollouts and evaluate exploration on the data collected by these rollouts. The data collected by these rollouts is not used for learning. In addition to measure changes in exploration more quickly, this allows us to assess state space coverage properties of the exploratory policy with greater statistical robustness by simply performing my rollouts.

3.6 State Space Coverage

We assess exploration in terms of state space coverage. We assume that the environment states s are $s \in \mathcal{R}^d$ and that the states have finite upper and lower limits: $s \in [\text{low}, \text{high}]$, $\text{low}, \text{high} \in \mathcal{R}^d$. We investigate four measures: X_{bin} , X_{Urel} , X_{BBM} , X_{NN} , which are illustrated in Figure 3.

The most intuitive measure for state-space coverage is a histogram based approach X_{bin} , which divides the state-space into equally many bins along each dimension and measures the ratio of non-empty bins to the total number of bins.

$$X_{\text{bin}} = \frac{\# \text{ of non empty bins}}{\# \text{ number of bins}} \quad (5)$$

Since the number of bins, as the product of divisions along each dimension, grows exponentially with the dimensionality, the required number of data points becomes prohibitively large very quickly and alternatives are necessary.

Zhan et al. (2019) proposed two state-space coverage measures that also work well in high-dimensional spaces: the *bounding box mean* X_{BBM} , and the *nuclear norm* X_{NN} .

X_{BBM} measures the spread of the data. The bounding box mean (Zhan et al., 2019)

creates a d dimensional bounding box around the collected data $D = \{\dots, s^{(j)}, \dots\}$ and measures the mean of the side-lengths of this bounding box:

$$X_{\text{BBM}} = \frac{1}{d} \sum_i^d \left[\max_j s_i^{(j)} - \min_j s_i^{(j)} \right] \quad (6)$$

X_{NN} , the nuclear norm (Zhan et al., 2019) estimates the covariance matrix C of the data and measures data spread by the trace, the sum of the eigenvalues of the estimated covariance:

$$X_{\text{NN}}(D) := \text{trace}(C(D)) \quad (7)$$

As we will see, extreme values or values close to the state space boundaries can lead to over-estimation of the state space coverage by these two measures. We therefore propose a measure more suitable to higher dimensions: $X_{\text{Urel}}(D)$. the Uniform-relative-entropy X_{Urel} , measure assesses the uniformity of the collected

data, by measuring the exploration as the symmetric divergence between a uniform prior over the state space U and the data distribution Q_D :

$$X_{\mathcal{U}\text{rel}}(D) = -D_{\text{KL}}(U||Q_D) - D_{\text{KL}}(Q_D||U) \quad (8)$$

since Q_D is only available through estimation, D_{KL} is estimated using the nearest-neighbor-ratio-estimator (Noshad et al., 2017). The inspiration for this measure comes from the observation that the exploration reward for count-based methods without task-reward would be maximized by a uniform distribution. We assume that for robotics tasks reasonable bounds on the state space can be found. In a bounded state space, the uniform distribution is the least presumptive (maximum entropy) distribution.

Estimation of $X_{\mathcal{U}\text{rel}}$, kNN estimator: One possible estimator for $\hat{q}(s)$ is a k-Nearest-Neighbor (kNN) density estimator (Bishop, 2006), where V_d denotes the unit volume of a d -dimensional sphere, $R_k(x)$ is the Euclidean distance to the k -th neighbor of x , and n is the total number of samples in \mathcal{D} :

$$V_d = \frac{\pi^{d/2}}{\Gamma(\frac{d}{2} + 1)} \quad (9)$$

$$\hat{q}_k(x) = \frac{k}{n} \frac{1}{V_d R_k(x)^d} = \frac{k}{n V_d} \frac{1}{R_k(x)^d} \quad (10)$$

where Γ denotes the gamma-function.

Estimation of $X_{\mathcal{U}\text{rel}}$, NNR estimator: Noshad et al. (Noshad et al., 2017) proposed an f -divergence estimator, the Nearest-Neighbor-Ratio (NNR) estimator, based on the ratio of the nearest neighbors around a query point, which we will use to estimate the KL-divergence.

They state that this estimator has a couple of beneficial properties. Among these, the most important property for our metric is not being affected by the over- / under-estimation artifacts of the kNN estimator close to the boundaries of the state space.

For the general case of estimating $D_{\text{KL}}(P||Q)$, we take samples from $X \sim Q$ and $Y \sim P$. Let $\mathcal{R}_k(Y_i)$ denote the set of the k -nearest neighbors of Y_i in the set $Z := X \cup Y$. N_i is the number of points from $X \cap \mathcal{R}_k(Y_i)$, M_i is the number of points from $Y \cap \mathcal{R}_k(Y_i)$, M is the number of points in Y and N is the number of points in X , $\eta = \frac{M}{N}$, and C_L and C_U are the lower and upper limits of the densities P and Q . Then,

$$D_{\text{KL}}(P||Q) \approx \hat{D}_g(X, Y) \quad (11)$$

$$\hat{D}_g(X, Y) := \max \left(\frac{1}{M} \sum_{i=1}^M \hat{g}\left(\frac{\eta N_i}{M_i + 1}, 0\right) \right) \quad (12)$$

$$\hat{g}(x) := \max(g(x), g(C_L/C_U)) \quad (13)$$

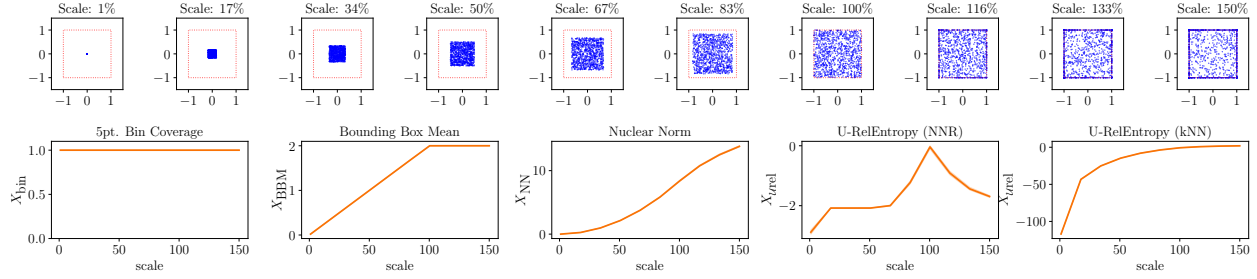
$$g(\rho) := -\log(\rho) \quad (14)$$

3.6.1 Evaluation of Measures on Synthetic Data

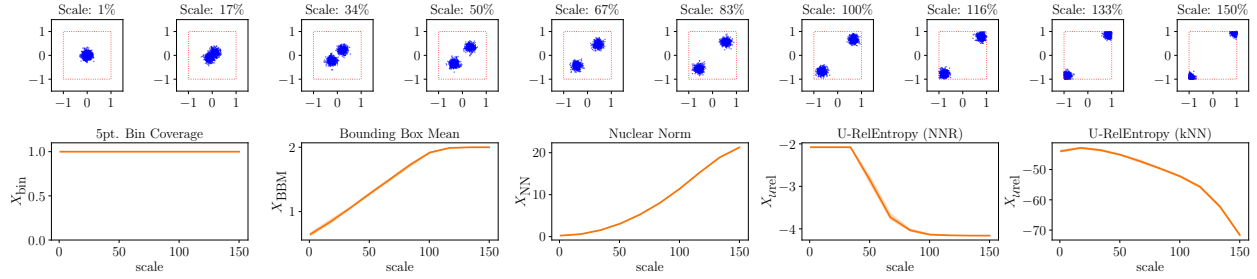
To compare the different exploration metrics, we assumed a $d = 25$ -dimensional state space, generated data from two different types of distributions, and compared the exploration metrics on these data. The experiments were repeated 10 times, and the mean and min-max values are plotted.

The inspiration of the first case would be an agent, for example a robot arm, that is stuck in the joint limits for at least some joints, and moving along those limits. The second example highlights that if the agent would set off in two opposite directions and then be stuck at these two opposing limits.

These two cases are depicted in Figure 4. While the data are d -dimensional, they come from factorial distributions, similarly distributed along each dimension. Thus, we can gain intuition about the distribution from scatter plots of the first vs. second dimension. This is depicted at the top of each of the two parts. The bottom part of each comparison shows the different exploration metrics, where the scale parameter is depicted on the x axis and the exploration measure on the y axis.



(a) Growing Uniform distribution: evaluation of the state-space coverage measures on synthetic data – for larger scale values more points are clipped to the state space boundaries, leading to an expected decrease in state space coverage for scales larger than 100%. First two dimensions of factorized 25 dimensional data are shown.



(b) Growing Distance of Modes of 2-Mixture of Truncated Normal: evaluation of the state-space coverage measures on synthetic data. For larger scale values, the location of the mixture components is closer to the boundary – leading to an expected reduce in coverage for larger scale values. First two dimensions of factorized 25 dimensional data are shown.

Figure 4: Comparison of exploration metrics on different data generating distributions dependent on one *scale* parameter: 25 dimensional factorial distributions, similarly distributed along each dimension. The scatter plots depict first vs. second dimension (a-b, top). Each comparison (a-b, bottom) shows the different exploration metrics X_{bin} , X_{BBM} , X_{NN} and X_{Urel} (ours) on the *y* axis and the scale parameter is depicted on the *x* axis.

(a) Growing Uniform: Figure 4(a) depicts data generated by a uniform distribution, centered around the middle of the state space, with minimal and maximal values growing relatively to the full state space according to the *scale* parameter from 1% to 150%. Since in the latter case, many points would lie outside the allowed state space; these values are clipped to the state space boundaries. This loosely corresponds to an undirected exploring agent that overshoots and hits the state space limits, sliding along the state-space boundaries. Note how the estimation (kNN vs. NNR) has a great impact on the X_{Urel} metric’s performance here: We would expect a maximum around a scale of 100% and smaller values before and after (due to clipping). Here the X_{Urel} (NNR) metric most closely follows this expectation. The true divergence would follow a similar shape although with more extreme values.

(b) Bi-Modal Truncated Normal moving locations: Figure 4(b) shows a mixture of two truncated Gaussian distributions, with equal standard deviations but located further and further apart (depending on the scale parameter). In this case, the state space coverage should increase until both distributions are sufficiently apart, should then stay the same, and begin to drop as the proximity to the state space limits the points to an ever smaller volume. While somewhat contrived, it highlights difficulties in the exploration metrics. Both the bounding-box mean X_{BBM} and the nuclear norm X_{NN} completely fail to account for vastly unexplored areas between the extreme points.

Since the X_{Urel} NNR metric is clipped (by definition of NNR) the metric reaches its limits when the density ratios become extreme, which presumably happens for very small and large scale parameters in this setting. Here the X_{Urel} kNN appears to outperform NNR even though it also suffers from under-estimation of the divergence for points close to the boundaries.

The experiments on synthetic data showed that the histogram based measure is not useful in high-dimensional spaces. The alternatives X_{BBM} and X_{NN} are susceptible to artifacts on bounded support. This susceptibility

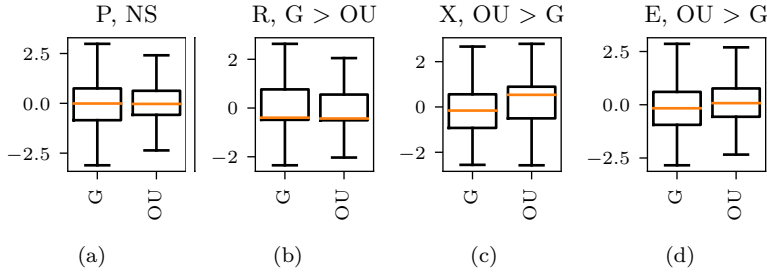


Figure 5: Comparison of standardized measures (P, X, R, E), for the two noise types. Values are standardized to control for and aggregate over algorithm, environment and noise-scale. (a) Evaluation Performance (P), difference is not significant, (b) Returns collected under the exploration policy (R), Gaussian noise appears to collect data with slightly better ($\alpha = 0.01$) returns, (c) state space coverage of the exploratory policy (X), (d) state space coverage of evaluation rollouts (E). Gaussian noise leads to slightly higher exploratory returns (R) while OU leads to higher exploratory state-space coverage (X).

to boundary artifacts is also present in the kNN-based $X_{\mathcal{U}_{\text{rel}}}$ estimator, because of these results we employ the NNR-estimator based $X_{\mathcal{U}_{\text{rel}}}$ in the rest of this paper and refer to it as $X_{\mathcal{U}_{\text{rel}}}$ (X).

4 Results: What action noise to use?

In this section we analyze the data collected in the experiments described in the previous section. We first look at the experiments performed under a constant scale scheduler since this is the most common case in the literature. In this setting we will look at two aspects: first, is one of the two action noise types generally superior to the other (*Q1*)? And secondly, is there a generally preferable action noise scale (*Q2*)? Then, we will compare across constant, linear and logistic schedulers to see if reducing the noise impact over the training process is a reasonable thing to do (*Q3*), finally we compare the relative importance of the scheduler, noise-type and scale (*Q4*).

4.1 (Q1) Which action noise-type to use? (and what are the impacts)

To compare for the type of action noise, we proceed as follows, we group and standardize the aggregated performance and exploration results (see sec 3.5 that describes how data is aggregated over training process) by algorithm, environment, and action-noise scale. Then we aggregate the results depending on the noise type across the normalized results. Figure 5 illustrates the results. The results indicate no significant difference (t-test, $\alpha = 0.01$) in evaluation performance (P) of the policies for both noise-types.

However, looking at the data collected with the exploratory policy (R), we see slightly but statistically significantly higher returns for Gaussian noise compared to OU noise. In case of the state-space coverage of the exploratory policy (X) measured by $X_{\mathcal{U}_{\text{rel}}}$, the difference is even more pronounced but reversed. This indicates that even if there are statistically significantly differences between the noise types in (R) and (X) this does not necessarily translate into changes of the evaluation performance of the learned policy (P). The results indicate that, most generally, neither of the two noise types can readily be preferred above the other. Note that all the values here are standardized, thus all the values appear to have similar ranges. (See Figure B.1 per environment results.) Compared to this, Table 3 breaks down the results per environment and shows that depending on the environment either Gaussian (G), or Ornstein-Uhlenbeck (OU) can outperform (t-test, $\alpha = 0.1$) the other unless they perform equally well (NS, not significant). In most environments, OU noise increases exploratory state space coverage (X), apart from the Hopper environment where wrong actions can lead to failure and thus end the episode prematurely. For most environments the exploratory returns (R) are higher for Gaussian noise, which we can see, does not necessarily translate to a better learned performance (P) (e.g. apart from the Reacher environment). In this more detailed view, we see that, while generally both noise-types appear to perform equally well, this is not the case if we look on a per-environment level. We also see that Gaussian noise appears to improve exploratory returns but Ornstein-Uhlenbeck noise is more effective at increasing state space coverage.

Environment	P	d_P	R	d_R	X	d_X	E	d_E
Half-Cheetah	-	-	G > OU	0.22	OU > G	0.21	-	-
Hopper	OU > G	0.27	G > OU	0.29	G > OU	0.41	-	-
Inverted-Pendulum-Swingup	-	-	G > OU	1.15	OU > G	1.22	G > OU	0.22
Mountain-Car	OU > G	0.47	OU > G	0.66	OU > G	0.34	OU > G	0.71
Reacher	G > OU	0.87	G > OU	0.80	OU > G	1.01	OU > G	0.84
Walker2D	-	-	G > OU	0.18	OU > G	0.46	-	-

Table 3: Comparison of standardized measures (P, X, R, E), for the two noise types, per environment. Values are standardized to control for and aggregate over algorithm, and noise-scale. Significantly better noise type for each environment and measure is reported (one tailed t-test, $\alpha = 0.01$) along Cohen-d effect size. While overall neither of the two noise types leads to significantly better performance (P) (see Figure 5), per environment noise-type difference is significant. Shows whether Ornstein-Uhlenbeck (OU) or Gaussian (G) noise is (significantly) better for an environment. (significantly) better for an environment.

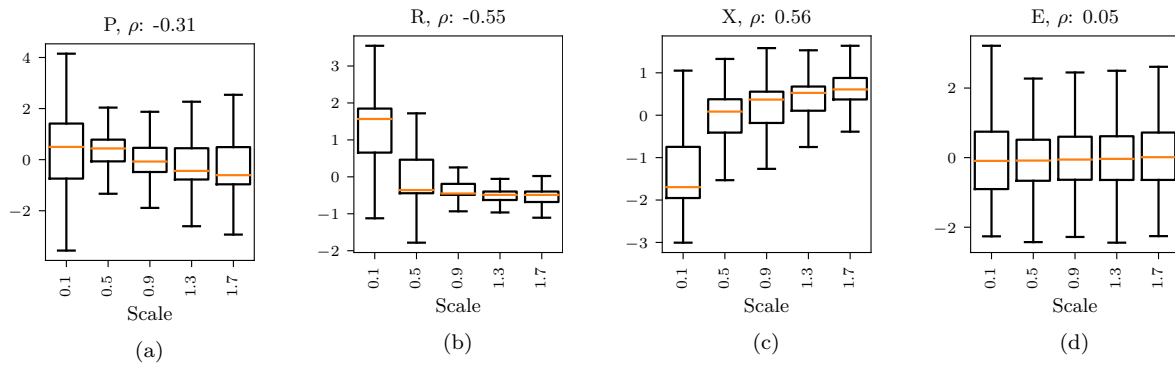


Figure 6: Comparison of standardized measures (P, X, R, E), against noise scales. Values are standardized to control for and aggregate over algorithm, environment and noise-type. (a) Evaluation Performance (P), appears negatively correlated with action noise scale ($\rho = -0.26$), (b) larger noise scales correlate with smaller returns collected under the exploration policy (R), (c) increasing the noise scale increases state space coverage of the exploratory policy (X), (d) state space coverage of evaluation rollouts (E).

4.2 (Q2) Which action noise scale to use?

To analyze which action noise scale to use, we first compare the scales across algorithms, environments and noise-types. These results are shown in Figure 6. The result in Figure 6 (a) shows the aggregated evaluation performance (P) with respect to each noise scale. A slight negative tendency is visible in the box plot and also indicated by the negative Spearman correlation coefficient of -0.26 . In Figure 6 (b), it appears that larger noise-scales reduce the exploratory returns (R). The correlation coefficient between (R) and the noise scale is even stronger: $\rho = -0.54$. If we look at the state-space-coverage of the exploratory policy (X), Figure 6 (c), the results indicate, that generally, larger noise-scales increase state coverage ($\rho = 0.62$).

Looking at the results on a per-environment level again reveals a more nuanced picture. Table 4 lists various Spearman correlation coefficients, both over all results and on a per-environment basis. To a large extend, the evaluation performance (P) is strongly correlated with the exploratory returns (R). Intuitively this makes sense, since it is easier to learn from data of higher quality. This is in line with findings from the Offline-RL literature, showing learning from expert data to be easier than learning from data of mixed-quality (Fu et al., 2020). We see a large correlation between state space coverage and then noise scale, which indicates, that the problem of insufficient exploration as lack of state space coverage can be remedied by increasing the action noise scale. In addition, however, we see a weaker but mostly negative correlation between the evaluation performance (P) and the noise-scale.

Environment	P/R	P/X	P/noise-scale	R/X	R/noise-scale	X/noise-scale
All	0.57	-0.03	-0.31	-0.30	-0.55	0.56
Half-Cheetah	0.22	-0.28	-0.35	-0.64	-0.74	0.75
Hopper	0.69	0.15	-0.87	0.27	-0.74	-0.17
Inverted-Pendulum-Swingup	-0.15	0.23	0.27	-0.88	-0.83	0.77
Mountain-Car	0.94	0.87	0.58	0.76	0.37	0.75
Reacher	0.84	-0.88	-0.56	-0.96	-0.84	0.69
Walker2D	0.76	-0.44	-0.81	-0.52	-0.82	0.63

Table 4: Spearman correlation coefficients per environment and across all environments. A general trend towards positive correlation between exploratory returns (R) and evaluation performance (P) can be observed. For some environments, exploratory state space coverage (X) is beneficial, while generally it is associated with decreased evaluation performance (P). Generally, increasing the noise-scale increases state-space coverage (X) but reduces exploratory returns (R).

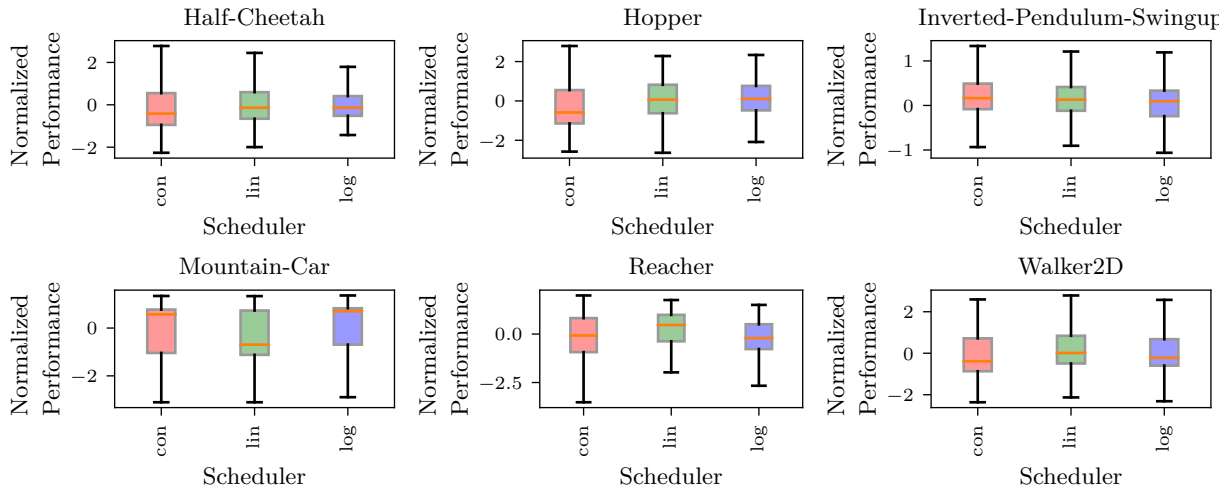


Figure 7: Comparison of the learned policy performance against schedulers, for each environment. Data is standardized to control for algorithm, and environment (but not noise-scale and -type). Overall, the linear and logistic schedulers perform equally well or better than the constant scheduler, while the constant scheduler does not show performance better than the other schedulers.

Interesting in this respect are the Mountain-Car and Inverted-Pendulum-Swingup environments. In the first, increasing the scale and thus the exploration is beneficial, while in the latter, higher exploratory returns appear to impact learned performance negatively. Both these systems are underactuated, and part of the solution is to inject energy into the system to get closer to the goal region. This underlines that *prior knowledge* on the task should guide the selection of the noise configuration.

4.3 (Q3) Should we scale down the noise over the training process?

The previous sections indicated that there is no unique solution for the best noise-type and that this choice is dependent on the environment. The analysis of the noise scale showed an overall preference for smaller noise-scales, but also showed that, in contrast, some environments require more noise to be solved successfully. In this section we analyze schedulers to reduce the influence of action-noise over the training progress.

Figure 7 shows the performance for each environment and each scheduler. The data is normalized by environment and algorithm before aggregation. The general trend observed across environments is that, when the environment reacts negatively to larger exploration (Table 4), reducing the noise over time improves

noise-scheduler	envname	(var, > con)	(var, > lin)	(var, > log)	count	(P, > con)	(P, > lin)	(P, > log)
constant_schedule	HalfCheetahPyBulletEnv-v0	-	NS	NS	800	-	NS	NS
	HopperPyBulletEnv-v0	-	NS	NS	800	-	NS	NS
	InvertedPendulumSwingupPyBulletEnv-v0	-	NS	NS	800	-	NS	Yes
	MountainCarContinuous-v0	-	Yes	NS	800	-	Yes	NS
	ReacherPyBulletEnv-v0	-	NS	NS	800	-	NS	NS
	Walker2DBulletEnv-v0	-	NS	NS	800	-	NS	NS
linear_schedule	HalfCheetahPyBulletEnv-v0	Yes	-	NS	800	Yes	-	NS
	HopperPyBulletEnv-v0	Yes	-	NS	800	Yes	-	NS
	InvertedPendulumSwingupPyBulletEnv-v0	NS	-	NS	800	NS	-	NS
	MountainCarContinuous-v0	NS	-	NS	800	NS	-	NS
	ReacherPyBulletEnv-v0	Yes	-	NS	800	Yes	-	Yes
	Walker2DBulletEnv-v0	Yes	-	NS	800	Yes	-	Yes
logistic_schedule	HalfCheetahPyBulletEnv-v0	Yes	Yes	-	800	Yes	NS	-
	HopperPyBulletEnv-v0	Yes	Yes	-	800	Yes	NS	-
	InvertedPendulumSwingupPyBulletEnv-v0	NS	NS	-	800	NS	NS	-
	MountainCarContinuous-v0	Yes	Yes	-	800	Yes	Yes	-
	ReacherPyBulletEnv-v0	Yes	NS	-	800	NS	NS	-
	Walker2DBulletEnv-v0	Yes	NS	-	800	Yes	NS	-
constant_schedule	Sum	0	1	0	0	0	1	1
linear_schedule	Sum	4	0	0	0	4	0	2
logistic_schedule	Sum	5	3	0	0	4	1	0

Table 5: Shows whether for each environment and scheduler: is the scheduler outperforming the other schedulers in terms of evaluation performance (P) (t-test, $\alpha = 0.01$) or variance of (P) (Levene’s test, $\alpha = 0.01$) Values are standardized to control for algorithm, noise-type and noise-scale.

performance. The reverse effect appears to be less important: for the environments that actually benefit from larger noise scales the constant scheduler does not outperform the linear and logistic schedulers.

Table 5 lists results on whether either constant, linear or logistic schedulers lead to *a*) significantly different (Levene, $\alpha = 0.5$) and (smaller) variance , and *b*) whether they lead to significantly improved (t-test, $\alpha = 0.1$) evaluation performance compared to the other schedulers.

This is indicated by *Yes*, *No* and *NS* for *not significant*. The lines under “sum” list how often we see positive results for each scheduler across all environments. The sum comparison shows a preferable result for linear and logistic schedulers compared to the constant scheduler across environments, both for reduction of variance as well as improvement of performance. The intuition on why linear and logistic outperform constant, and not the other way around is that, if we choose a large noise scale (that would force the data collection to be too off-policy), the scheduler can remedy this by reducing the impact of the noise. This in turn, then allows for a larger noise scale to be selected in the first place, which has a beneficial effect if the system requires more noise to be pushed out of a local optimum. If the environment benefits from a small noise-scale, further reducing the noise does not have a huge impact and the change of scaling down a large noise-scale (e.g. 1.3) is greater than the effect of scaling down a small noise-scale (e.g. 0.1).

4.4 (Q4) How important are the different parameters?

In the previous sections we looked at each noise-configuration parameter independently, but the question remains whether all the parameters are equally important or which parameter is the most important. We standardize results to control for environment and algorithm, and different to sections (Q1) and (Q2), which looked at the commonly applied setting of a constant-noise scale, in this section we compare across noise-scheduler settings.

Table 6 shows the ANOVA partial- η^2 results for scheduler, scale, type. The results indicate that action noise-scale is the most important factor for the majority of environments, apart from the Reacher environment where noise-type is most important (small effect $\eta^2 \geq 0.01$, medium effect $\eta^2 \geq 0.06$, large effect $\eta^2 \geq 0.14$). The columns R(P/X), R(P/sigma), and R(P/R) indicate the Spearman correlation coefficients (significant with $\alpha = 0.01$, not-significant coefficients are omitted)

The correlation coefficients for evaluation performance (P) vs. exploration state-space coverage (X) and noise-scale (sigma) agree: a larger noise scale induces larger-state-space coverage. The results show that this

envname	R(P/X)	R(P/sigma)	R(P/R)	eta2 scheduler	eta2 type	eta2 scale
all	-0.479	-0.112	0.790	0.006	0.000	0.071
Mountain-Car	0.656	0.463	0.955	0.051	0.117	0.324
Inverted-Pendulum-Swingup	-	0.119	0.150	0.004	0.008	0.085
Reacher	-0.865	-0.306	0.768	0.092	0.415	0.270
Hopper	-0.411	-0.588	0.696	0.240	0.156	0.738
Walker2D	-0.678	-0.513	0.715	0.079	0.102	0.672
Half-Cheetah	-0.566	-0.269	0.770	0.008	0.004	0.170

Table 6: Correlation coefficients and ANOVA partial- η^2 effect sizes for the factors: scheduler, type and scale. Results are shown across all environments (standardized and controlled for environment and algorithm), and per environment (standardized and controlled for algorithm). Generally, exploratory returns (R) and evaluation performance (P) are positively associated, while generally larger state-space coverage (X) appears to impact performance (P) negatively. Noise-scale accounts for larger variance than scheduler or type.

envname	noise-scheduler	noise-scale	noise_type	Horizon	Recommendation
all	lin/log	0.5	ou		
Mountain-Car	log	1.7	ou	L	large, OU
Inverted-Pendulum-Swingup	con/lin/log	0.5/0.9/1.3/1.7	gauss	L	large
Reacher	lin	0.1/0.5	gauss	-	Gauss, small, sched
Hopper	log	0.1	ou	S	small
Walker2D	lin	0.1	ou	S	small, OU, sched
Half-Cheetah	lin/log	0.5	gauss/ou	S	small

Table 7: Comparison of best-ranked noise-type, -scale and -scheduler across all and for each environment. Scheduler, type and scale are investigated separately by standardizing the values to control for environment, algorithm and the respective other two factors. Horizon indicates whether we expect a long or short effective planning horizon, while recommendation indicates configuration choices in order of importance as per Table 6.

also holds when compared across the three noise-schedulers. Overall, across environments and schedulers, we see a strong correlation between the exploration-policy returns (R) and evaluation performance (P).

5 Discussion

The experiments conducted in this paper showed that the action noise does, depending on the environment, have a *significant* impact on the evaluation performance of the learned policy (Q1). Which action noise type is best, unfortunately *depends on the environment*.

For the action noise scale (Q2), our results have shown, that generally a larger noise scale increases state space coverage.

But since for many environments, learning performance is negatively associated with larger state space coverage, a large noise scale does not have a preferable impact. Similarly, very small scales also appear not to have a preferable impact, as they appear to increase variance of the evaluation performance Figure 6.

It is difficult to draw general conclusions from a limited set of environments and extending the evaluation is limited by the prohibitively large computational costs. However, we would like to provide observations that may guide the search for the right action noise.

Table 7 shows the best ranking scheduler, scale and type configurations for each, and across environments. The ranking is based on the count of significantly better comparisons (pair-wise one-sided Tukeys HSD, $\alpha = 0.01$). For each of scheduler, type and scale we standardize to control for the other two factors.

Intuitively, the locomotion environments require only a short actual planning horizon: the reward in the environments is based on the distance moved and is relevant as soon as the locomotion pattern is repeated,

for example a 30 step horizon is enough for similar locomotion benchmarks (Pinneri et al., 2020). Differently, the Mountain-Car environment only provides informative reward at the end of a successful episode. Similar, the Inverted-Pendulum-Swingup uses a shaped reward, that does not account for spurious local optima: to swing-up and increase system energy, the distance to the goal has to be increased again. These observations are indicated in the column *Horizon*. Finally, the recommendation column interprets the best-ranked results under the observed importance (Q4) reported in Table 6.

Given these results, we provide the following intuitions as a starting point for optimizing the action-noise parameters:

under-actuation \triangleright more state space coverage We found that in the case of the Mountain-Car and the Inverted-Pendulum-Swingup, both of which are underactuated tasks and requiring a swinging up phase, larger state-space coverages or larger action-noise scales appear beneficial (Table 4 and Table 6). Intuitively, under-actuation implies harder-to-reach state-space areas.

misleading reward \triangleright more state space coverage Actions are penalized in the Mountain Car by an action-energy penalty, which means not performing any action forms a local optimum. In the case of the Inverted-Pendulum-Swingup, the distance to the goal forms a shaped reward. However, when swinging up, increasing the distance to the goal is necessary. Thus, the shaped reward can be misleading and optimizing for the reward too greedily moves the agent away from taking necessary steps. Optimizing for a spurious local optimum implies not reaching areas of the state-space where the actual goal would be found, thus the state space coverage needs to be increased to find these areas.

shorter horizon \triangleright less state space coverage The environments Hopper, Reacher, Walker2D model locomotion tasks with repetitive movement sequences. In the Mountain-Car, positive reward is only achieved at the successful end of the episode, where as in the locomotion tasks positive reward is retrieved after each successful cycle of the locomotion pattern. Thus effectively the required planning horizon is shorter compared to tasks such as the Mountain-Car. Consistently with the previous point, if the effective horizon is shorter, the rewards are shaped more efficiently, we see negative correlations with the state space coverage and the noise scale: if the planning horizon is shorter, the reward can be optimized more greedily, meaning the state space coverage can be more focused and thus smaller.

more state space coverage \triangleright larger scale Our analysis showed that, to increase state space coverage, one remedy is to increase the scale of the action noise, thereby leading to a higher probability of taking larger, i.e. further away from the middle of the action space, actions. In continuous control domains actions are typically related to position, velocity or torque control. In position control, larger actions are directly related to more extreme positions in the state space. In velocity control, larger actions lead to moving away from the initial state more quickly. In torque control, larger torques lead to more energy in the system and larger velocities. Currently most policies in D-RL are either uni-modal stochastic policies, or deterministic policies. In both cases, larger action noise leads to a broader selection of actions and, by the fore-mentioned mechanism, to a broader state space coverage. Note that while this is the general effect we observed, it is also possible that a too large action can have a detrimental effect, e.g. the Hopper falling, and the premature end of the episode will lead to a reduction of the state space coverage.

more state space coverage \triangleright type of noise Depending on the environment dynamics, correlated noise (Ornstein-Uhlenbeck) can increase the state space coverage: for example, if the environment shows integrative behavior over the actions, temporally uncorrelated noise (Gaussian) leads to more actions that “undo” previous progress and thus less coverage.

less state space coverage, on-policy \triangleright scheduler to reduce noise If the policy is already sufficiently good, or the reward is shaped well enough, exploration should focus around good trajectories and thus, it makes sense to gradually reduce the impact of the noise (Q3) and gradually become “more on-policy”.

use a scheduler We found that using schedulers to reduce the impact of action noise over time, decreases variance of the performance, and thus makes the learning more robust, while also generally increasing the evaluation performance overall, presumably because, once a trajectory to the goal is found, more fine grained exploration around the trajectory is better able to improve performance.

6 Conclusion

In this paper we present an extensive empirical study on the impact of action-noise configurations. We compared the two most prominent action noise types: Gaussian and Ornstein-Uhlenbeck, different scale parameters (0.1, 0.5, 0.9, 1.3, 1.7), proposed a scheduled reduction of the impact of the action noise over the training progress and proposed a state-space coverage measure ($X_{U_{\text{rel}}}$) to assess the achieved exploration in terms of state-space coverage. We compared DDPG, TD3, SAC and a deterministic variant of SAC on the benchmarks: Mountain-Car, Inverted-Pendulum-Swingup, Reacher, Hopper, Walker2D, Half-Cheetah.

While we found that neither noise type is preferable across environments, we did find, that, depending on the environment there is a *significant difference* between the two *noise types*. We found that the evaluation returns (P) are (often strongly) correlated with, but are not exactly determined by, the returns of the exploratory policy (R): A large gap in (R) does not necessarily imply a large gap in (P) and vice versa. The interpretation of this finding is that, when optimizing *exploration parameters*, (R) is a good predictor of (P), but it is not the only determining factor. We also found that the exploratory policy's state-space coverage (X) is (often strongly) correlated with the evaluation returns (P) and depending on the environment, positively or negatively. This suggests, that, when optimizing exploration parameters the exploratory-state-space coverage and especially the environment dependent *sign of the correlation* need to be considered. To our surprise, we found that for most environments the impact of the *noise-scale* is *larger* than the impact of *noise-type*. We synthesized our results into a set of *heuristics* on how to choose the action noise based on the properties of the environment. Finally and most importantly, we recommend a *scheduled reduction* of the impact of action noise over the training progress.

References

Scott Fujimoto, Herke van Hoof, and David Meger. Addressing Function Approximation Error in Actor-Critic Methods. In *International Conference on Machine Learning*, pages 1587–1596. PMLR, October 2018.

Timothy P. Lillicrap, Jonathan J. Hunt, Alexander Pritzel, Nicolas Heess, Tom Erez, Yuval Tassa, David Silver, and Daan Wierstra. Continuous control with deep reinforcement learning. In *Proc. 4th Int. Conf. Learning Representations, (ICLR)*, 2016.

Eric Liang, Richard Liaw, Philipp Moritz, Robert Nishihara, Roy Fox, Ken Goldberg, Joseph E. Gonzalez, Michael I. Jordan, and Ion Stoica. RLlib: Abstractions for Distributed Reinforcement Learning. *arXiv:1712.09381 [cs]*, June 2018.

Antonin Raffin, Ashley Hill, Adam Gleave, Anssi Kanervisto, Maximilian Ernestus, and Noah Dormann. Stable-baselines3: Reliable reinforcement learning implementations. *Journal of Machine Learning Research*, 22(268):1–8, 2021a.

Yasuhiro Fujita, Prabhat Nagarajan, Toshiki Kataoka, and Takahiro Ishikawa. ChainerRL: A Deep Reinforcement Learning Library. *Journal of Machine Learning Research*, 22(77):1–14, 2021. ISSN 1533-7928.

Takuma Seno and Michita Imai. D3rlpy: An Offline Deep Reinforcement Learning Library. *arXiv:2111.03788 [cs]*, November 2021.

Andrew William Moore. Efficient memory-based learning for robot control. 1990.

Tuomas Haarnoja, Aurick Zhou, Kristian Hartikainen, George Tucker, Sehoon Ha, Jie Tan, Vikash Kumar, Henry Zhu, Abhishek Gupta, Pieter Abbeel, and Sergey Levine. Soft Actor-Critic Algorithms and Applications. *arXiv:1812.05905 [cs, stat]*, January 2019.

Antonin Raffin. RL baselines3 zoo. *GitHub repository*, 2020.

Itai Caspi, Gal Leibovich, Shadi Endrawis, and Gal Novik. Reinforcement Learning Coach. Zenodo, December 2017.

Matt Hoffman, Bobak Shahriari, John Aslanides, Gabriel Barth-Maron, Feryal Behbahani, Tamara Norman, Abbas Abdolmaleki, Albin Cassirer, Fan Yang, Kate Baumli, Sarah Henderson, Alex Novikov, Sergio Gómez Colmenarejo, Serkan Cabi, Caglar Gulcehre, Tom Le Paine, Andrew Cowie, Ziyu Wang, Bilal Piot, and Nando de Freitas. Acme: A Research Framework for Distributed Reinforcement Learning. *arXiv:2006.00979 [cs]*, June 2020.

Greg Brockman, Vicki Cheung, Ludwig Pettersson, Jonas Schneider, John Schulman, Jie Tang, and Wojciech Zaremba. OpenAI Gym. *arXiv:1606.01540 [cs]*, June 2016.

Erwin Coumans and Yunfei Bai. PyBullet, a Python module for physics simulation for games, robotics and machine learning. 2016.

Benjamin Ellenberger. PyBullet gymperium. *GitHub repository*, 2018.

Volodymyr Mnih, Koray Kavukcuoglu, David Silver, Andrei A. Rusu, Joel Veness, Marc G. Bellemare, Alex Graves, Martin Riedmiller, Andreas K. Fidjeland, Georg Ostrovski, Stig Petersen, Charles Beattie, Amir Sadik, Ioannis Antonoglou, Helen King, Dharshan Kumaran, Daan Wierstra, Shane Legg, and Demis Hassabis. Human-level control through deep reinforcement learning. *Nature*, 518(7540):529–533, February 2015. ISSN 0028-0836, 1476-4687. doi: 10.1038/nature14236.

Marc G. Bellemare, Yavar Naddaf, Joel Veness, and Michael Bowling. The arcade learning environment: An evaluation platform for general agents. *Journal of Artificial Intelligence Research*, 47:253–279, 2013.

Emanuel Todorov, Tom Erez, and Yuval Tassa. MuJoCo: A physics engine for model-based control. In *2012 IEEE/RSJ International Conference on Intelligent Robots and Systems*, pages 5026–5033, October 2012. doi: 10.1109/IROS.2012.6386109.

Yuval Tassa, Yotam Doron, Alistair Muldal, Tom Erez, Yazhe Li, Diego de Las Casas, David Budden, Abbas Abdolmaleki, Josh Merel, Andrew Lefrancq, Timothy Lillicrap, and Martin Riedmiller. DeepMind Control Suite. *arXiv:1801.00690 [cs]*, January 2018.

Dmitry Kalashnikov, Alex Irpan, Peter Pastor, Julian Ibarz, Alexander Herzog, Eric Jang, Deirdre Quillen, Ethan Holly, Mrinal Kalakrishnan, Vincent Vanhoucke, and Sergey Levine. QT-Opt: Scalable Deep Reinforcement Learning for Vision-Based Robotic Manipulation. June 2018.

Ronald J. Williams. Simple statistical gradient-following algorithms for connectionist reinforcement learning. *Machine learning*, 8(3-4):229–256, 1992.

Richard S Sutton, David McAllester, Satinder Singh, and Yishay Mansour. Policy Gradient Methods for Reinforcement Learning with Function Approximation. In *Advances in Neural Information Processing Systems*, volume 12. MIT Press, 1999.

John Schulman, Sergey Levine, Philipp Moritz, Michael Jordan, and Pieter Abbeel. Trust Region Policy Optimization. In *Proceedings of the 32Nd International Conference on International Conference on Machine Learning - Volume 37*, ICML’15, pages 1889–1897, Lille, France, 2015. JMLR.org.

John Schulman, Filip Wolski, Prafulla Dhariwal, Alec Radford, and Oleg Klimov. Proximal Policy Optimization Algorithms. *CoRR*, abs/1707.06347, 2017.

David Silver, Guy Lever, Nicolas Heess, Thomas Degris, Daan Wierstra, and Martin Riedmiller. Deterministic policy gradient algorithms. In *ICML*, 2014.

Zeping Zhan, Batu Aytemiz, and Adam M Smith. Taking the scenic route: Automatic exploration for videogames. In *KEG@ AAAI*, 2019.

Bogdan Mazoure, Thang Doan, Audrey Durand, Joelle Pineau, and R. Devon Hjelm. Leveraging exploration in off-policy algorithms via normalizing flows. In *Conference on Robot Learning*, pages 430–444. PMLR, May 2020.

Patrick Nadeem Ward, Ariella Smofsky, and Avishek Joey Bose. Improving Exploration in Soft-Actor-Critic with Normalizing Flows Policies. *arXiv:1906.02771 [cs, stat]*, June 2019.

Cristina Pinneri, Shambhuraj Sawant, Sebastian Blaes, Jan Achterhold, Joerg Stueckler, Michal Rolinek, and Georg Martius. Sample-efficient Cross-Entropy Method for Real-time Planning. *arXiv:2008.06389 [cs, stat]*, August 2020.

Horia Mania, Aurelia Guy, and Benjamin Recht. Simple random search provides a competitive approach to reinforcement learning. *arXiv:1803.07055 [cs, math, stat]*, March 2018.

Matthias Plappert, Rein Houthooft, Prafulla Dhariwal, Szymon Sidor, Richard Y. Chen, Xi Chen, Tamim Asfour, Pieter Abbeel, and Marcin Andrychowicz. Parameter space noise for exploration. *CoRR*, abs/1706.01905, 2017.

Antonin Raffin, Jens Kober, and Freek Stulp. Smooth Exploration for Robotic Reinforcement Learning. *arXiv:2005.05719 [cs, stat]*, June 2021b.

Yuri Burda, Harrison Edwards, Amos J. Storkey, and Oleg Klimov. Exploration by random network distillation. In *7th International Conference on Learning Representations, ICLR*, 2019.

Haoran Tang, Rein Houthooft, Davis Foote, Adam Stooke, OpenAI Xi Chen, Yan Duan, John Schulman, Filip DeTurck, and Pieter Abbeel. #Exploration: A Study of Count-Based Exploration for Deep Reinforcement Learning. In I. Guyon, U. V. Luxburg, S. Bengio, H. Wallach, R. Fergus, S. Vishwanathan, and R. Garnett, editors, *Advances in Neural Information Processing Systems 30*, pages 2753–2762. Curran Associates, Inc., 2017.

Mirco Mutti, Lorenzo Pratissoli, and Marcello Restelli. A Policy Gradient Method for Task-Agnostic Exploration. *arXiv:2007.04640 [cs, stat]*, July 2020.

Zhang-Wei Hong, Tzu-Yun Shann, Shih-Yang Su, Yi-Hsiang Chang, Tsu-Jui Fu, and Chun-Yi Lee. Diversity-driven exploration strategy for deep reinforcement learning. In *Advances in Neural Information Processing Systems*, pages 10489–10500, 2018.

Vitchyr H. Pong, Murtaza Dalal, Steven Lin, Ashvin Nair, Shikhar Bahl, and Sergey Levine. Skew-Fit: State-Covering Self-Supervised Reinforcement Learning. August 2020.

Ashley Hill, Antonin Raffin, Maximilian Ernestus, Adam Gleave, Rene Traore, Prafulla Dhariwal, Christopher Hesse, Oleg Klimov, Alex Nichol, Matthias Plappert, Alec Radford, John Schulman, Szymon Sidor, and Yuhuai Wu. Stable Baselines. *GitHub repository*, 2018.

Tim Seyde, Igor Gilitschenski, Wilko Schwarting, Bartolomeo Stellato, Martin Riedmiller, Markus Wulfmeier, and Daniela Rus. Is Bang-Bang Control All You Need? Solving Continuous Control with Bernoulli Policies. *arXiv:2111.02552 [cs]*, November 2021.

Morteza Noshad, Kevin R. Moon, Salimeh Yasaei Sekeh, and Alfred O. Hero. Direct estimation of information divergence using nearest neighbor ratios. In *2017 IEEE International Symposium on Information Theory (ISIT)*, pages 903–907, June 2017. doi: 10.1109/ISIT.2017.8006659.

Christopher M. Bishop. Pattern recognition. *Machine Learning*, 128:1–58, 2006.

Justin Fu, Aviral Kumar, Ofir Nachum, George Tucker, and Sergey Levine. D4RL: Datasets for Deep Data-Driven Reinforcement Learning. *arXiv:2004.07219 [cs, stat]*, June 2020.

Appendices

A Deterministic SAC

Algorithm A.1 (Deterministic) Soft Actor-Critic

```

Initialize parameter vectors  $\psi, \bar{\psi}, \theta, \phi$ .
for each iteration do
  for each environment step do
     $\mu_t, \sigma_t = f_\phi(s_t)$ 
     $\varepsilon_t \sim \mathcal{A}$                                  $\triangleright \mathcal{A} \dots$  action noise process
     $a_t = \mu_t + \varepsilon_t$                        $\triangleright$  DetSAC
     $\pi_\phi(\cdot|s_t) = \mathcal{N}(\cdot|\mu_t, \sigma_t)$        $\triangleright$  SAC
     $a'_t \sim \pi_\phi(a_t|s_t)$ 
     $a_t = a_t + \varepsilon_t$ 
     $s_{t+1} \sim p(s_{t+1}|s_t, a_t)$ 
     $\mathcal{D} \leftarrow \mathcal{D} \cup \{(s_t, a_t, r(s_t, a_t), s_{t+1})\}$ 
  end for
  for each gradient step do
    ... original SAC update (Haarnoja et al., 2019)
  end for
end for

```

B (Q1) Noise Type difference per environment

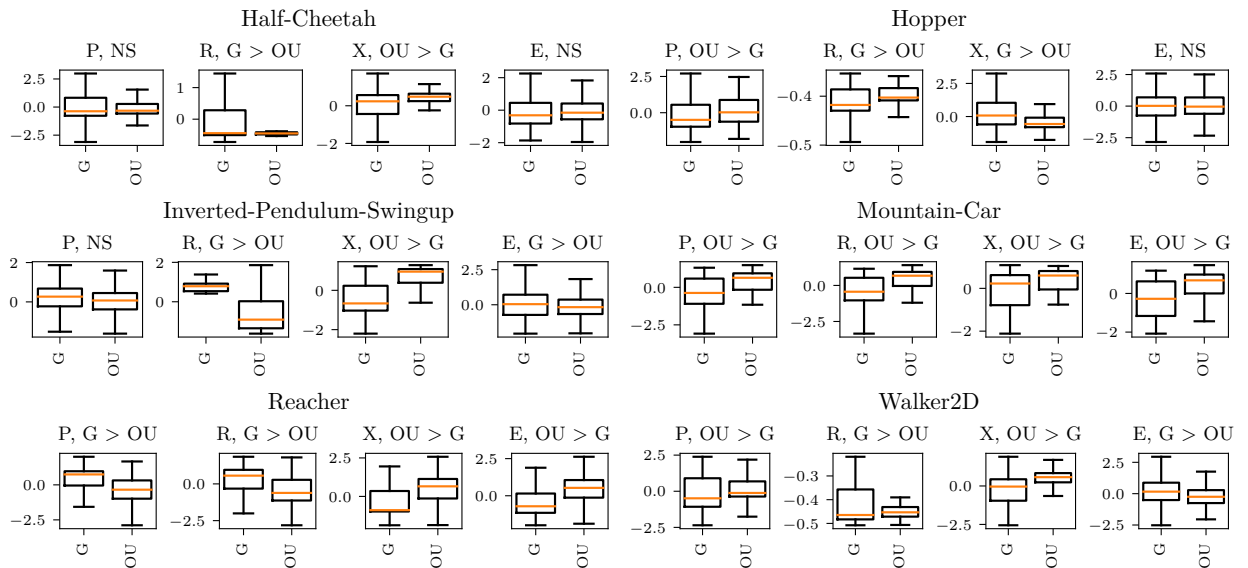


Figure B.1: Separate results for constant scheduler; comparison of noise type on P, R, X, E.

C Performed experiments

algorithm	envname	noise-scale	run											
			0.1	0.5	0.9	1.3	1.7	0.1	0.5	0.9	1.3	1.7	0.1	0.5
			gauss	gauss	gauss	gauss	gauss	ou						
ddpg	HalfCheetahPyBulletEnv-v0	constant_schedule	20	20	20	20	20	20	20	20	20	20	20	20
		linear_schedule	20	20	20	20	20	20	20	20	20	20	20	20
		logistic_schedule	20	20	20	20	20	20	20	20	20	20	20	20
	HopperPyBulletEnv-v0	constant_schedule	20	20	20	20	20	20	20	20	20	20	20	20
		linear_schedule	20	20	20	20	20	20	20	20	20	20	20	20
		logistic_schedule	20	20	20	20	20	20	20	20	20	20	20	20
	InvertedPendulumSwingupPyBulletEnv-v0	constant_schedule	20	20	20	20	20	20	20	20	20	20	20	20
		linear_schedule	20	20	20	20	20	20	20	20	20	20	20	20
		logistic_schedule	20	20	20	20	20	20	20	20	20	20	20	20
	MountainCarContinuous-v0	constant_schedule	20	20	20	20	20	20	20	20	20	20	20	20
		linear_schedule	20	20	20	20	20	20	20	20	20	20	20	20
		logistic_schedule	20	20	20	20	20	20	20	20	20	20	20	20
	ReacherPyBulletEnv-v0	constant_schedule	20	20	20	20	20	20	20	20	20	20	20	20
		linear_schedule	20	20	20	20	20	20	20	20	20	20	20	20
		logistic_schedule	20	20	20	20	20	20	20	20	20	20	20	20
	Walker2DBulletEnv-v0	constant_schedule	20	20	20	20	20	20	20	20	20	20	20	20
		linear_schedule	20	20	20	20	20	20	20	20	20	20	20	20
		logistic_schedule	20	20	20	20	20	20	20	20	20	20	20	20
detsac	HalfCheetahPyBulletEnv-v0	constant_schedule	20	20	20	20	20	20	20	20	20	20	20	20
		linear_schedule	20	20	20	20	20	20	20	20	20	20	20	20
		logistic_schedule	20	20	20	20	20	20	20	20	20	20	20	20
	HopperPyBulletEnv-v0	constant_schedule	20	20	20	20	20	20	20	20	20	20	20	20
		linear_schedule	20	20	20	20	20	20	20	20	20	20	20	20
		logistic_schedule	20	20	20	20	20	20	20	20	20	20	20	20
	InvertedPendulumSwingupPyBulletEnv-v0	constant_schedule	20	20	20	20	20	20	20	20	20	20	20	20
		linear_schedule	20	20	20	20	20	20	20	20	20	20	20	20
		logistic_schedule	20	20	20	20	20	20	20	20	20	20	20	20
	MountainCarContinuous-v0	constant_schedule	20	20	20	20	20	20	20	20	20	20	20	20
		linear_schedule	20	20	20	20	20	20	20	20	20	20	20	20
		logistic_schedule	20	20	20	20	20	20	20	20	20	20	20	20
	ReacherPyBulletEnv-v0	constant_schedule	20	20	20	20	20	20	20	20	20	20	20	20
		linear_schedule	20	20	20	20	20	20	20	20	20	20	20	20
		logistic_schedule	20	20	20	20	20	20	20	20	20	20	20	20
	Walker2DBulletEnv-v0	constant_schedule	20	20	20	20	20	20	20	20	20	20	20	20
		linear_schedule	20	20	20	20	20	20	20	20	20	20	20	20
		logistic_schedule	20	20	20	20	20	20	20	20	20	20	20	20
sac	HalfCheetahPyBulletEnv-v0	constant_schedule	20	20	20	20	20	20	20	20	20	20	20	20
		linear_schedule	20	20	20	20	20	20	20	20	20	20	20	20
		logistic_schedule	20	20	20	20	20	20	20	20	20	20	20	20
	HopperPyBulletEnv-v0	constant_schedule	20	20	20	20	20	20	20	20	20	20	20	20
		linear_schedule	20	20	20	20	20	20	20	20	20	20	20	20
		logistic_schedule	20	20	20	20	20	20	20	20	20	20	20	20
	InvertedPendulumSwingupPyBulletEnv-v0	constant_schedule	20	20	20	20	20	20	20	20	20	20	20	20
		linear_schedule	20	20	20	20	20	20	20	20	20	20	20	20
		logistic_schedule	20	20	20	20	20	20	20	20	20	20	20	20
	MountainCarContinuous-v0	constant_schedule	20	20	20	20	20	20	20	20	20	20	20	20
		linear_schedule	20	20	20	20	20	20	20	20	20	20	20	20
		logistic_schedule	20	20	20	20	20	20	20	20	20	20	20	20
	ReacherPyBulletEnv-v0	constant_schedule	20	20	20	20	20	20	20	20	20	20	20	20
		linear_schedule	20	20	20	20	20	20	20	20	20	20	20	20
		logistic_schedule	20	20	20	20	20	20	20	20	20	20	20	20
	Walker2DBulletEnv-v0	constant_schedule	20	20	20	20	20	20	20	20	20	20	20	20
		linear_schedule	20	20	20	20	20	20	20	20	20	20	20	20
		logistic_schedule	20	20	20	20	20	20	20	20	20	20	20	20
td3	HalfCheetahPyBulletEnv-v0	constant_schedule	20	20	20	20	20	20	20	20	20	20	20	20
		linear_schedule	20	20	20	20	20	20	20	20	20	20	20	20
		logistic_schedule	20	20	20	20	20	20	20	20	20	20	20	20
	HopperPyBulletEnv-v0	constant_schedule	20	20	20	20	20	20	20	20	20	20	20	20
		linear_schedule	20	20	20	20	20	20	20	20	20	20	20	20
		logistic_schedule	20	20	20	20	20	20	20	20	20	20	20	20
	InvertedPendulumSwingupPyBulletEnv-v0	constant_schedule	20	20	20	20	20	20	20	20	20	20	20	20
		linear_schedule	20	20	20	20	20	20	20	20	20	20	20	20
		logistic_schedule	20	20	20	20	20	20	20	20	20	20	20	20
	MountainCarContinuous-v0	constant_schedule	20	20	20	20	20	20	20	20	20	20	20	20
		linear_schedule	20	20	20	20	20	20	20	20	20	20	20	20
		logistic_schedule	20	20	20	20	20	20	20	20	20	20	20	20
	ReacherPyBulletEnv-v0	constant_schedule	20	20	20	20	20	20	20	20	20	20	20	20
		linear_schedule	20	20	20	20	20	20	20	20	20	20	20	20
		logistic_schedule	20	20	20	20	20	20	20	20	20	20	20	20
	Walker2DBulletEnv-v0	constant_schedule	20	20	20	20	20	20	20	20	20	20	20	20
		linear_schedule	20	20	20	20	20	20	20	20	20	20	20	20
		logistic_schedule	20	20	20	20	20	20	20	20	20	20	20	20

Table C.1: This table shows the number and configurations of independent learning experiments with different noise settings we use in this paper. Each run is performed from an independently, randomly drawn seed.